Steel and Composite Structures, *Vol. 27, No. 2 (2018) 177-184*
DOI: https://doi.org/10.12989/scs.2018.27.2.177

Topology optimization for thin plate on elastic foundations by using multi-material

Thien Thanh Banh [1a], Soomi Shin [2] and Dongkyu Lee [*1]

[1] *Department of Architectural Engineering, Sejong University, 209 Neungdong-ro, Gwangjin-gu, Seoul 05006, Republic of Korea*
[2] *Research Institute of Industrial Technology, Pusan National University, 2 Busandaehak-ro 63, Geumjeong-gu, Busan 46241, Republic of Korea*

(*Received September 23, 2017, Revised January 20, 2018, Accepted February 22, 2018*)

Abstract. This study contributes to evaluate multiphase topology optimization design of plate-like structures on elastic foundations by using classic plate theory. Multi-material optimal topology and shape are produced as an alternative to provide reasonable material assignments based on stress distributions. Multi-material topology optimization problem is solved through an alternative active-phase algorithm with Gauss-Seidel version as an optimization model of optimality criteria. Stiffness and adjoint sensitivity formulations linked to thin plate potential strain energy are derived in terms of multiphase design variables and Winkler-Pasternak parameters considering elastic foundation to apply to the current topology optimization. Numerical examples verify efficiency and diversity of the present topology optimization method of elastic thin plates depending on multiple materials and Winkler-Pasternak parameters with the same amount of volume fraction and total structural volume.

Keywords: topology optimization; multiphase; thin plate; adjoint sensitivity; elastic foundations; Winkler-Pasternak model

1. Introduction

Since the pioneering study by Bendsøe and Kikuchi (1988), topology optimization has made remarkable progress as an innovative numerical and design method, drawing an enormous amount of attention from the scientific community (Lee and Shin 2015, Vatanabe *et al*. 2016, Roodsarabi *et al*. 2016, Lee *et al*. 2015, 2017, Lee and Shin 2016). Due to significant advantages (Bendsøe and Sigmund 2004) of topology optimization, it has been widely utilized in designing mechanical components and in other engineering applications such as macro-structures (Liu *et al*. 2016a), laminated composite structures (Blasques and Stolpe 2012), lattice structures (Du *et al*. 2017), thermo-elastic structures (Xia and Wang 2008) and seismic analysis (Qiao *et al*. 2016).

Multi-material topology optimization is also an attractive issue in the field of structural topology optimization. In addition to inherit of main ideas of standard topology optimization, the optimal material distribution of variable densities is continuously derived. By using more additional stiff materials, topology optimization may produce structures with higher stiffness. It also offers material cost savings in compared with single material structures to arrive at required design performance. Zhou *et al*. (2007) introduced a phase field method for the multi-material structural topology optimization with a generalized Cahn-Hilliard model. Alonso *et al*. (2014) studied topology synthesis of multiple materials by using a multi Sequential Element Rejection and Admission (SERA) method. Liu *et al*. (2016b) presented an efficient multi-material topology optimization strategy for seeking the optimal layout of structures considering the cohesive constitutive relationship of the interface. Yun and Youn (2017) investigated optimized topologies using multiple materials for viscoelastically damped structures under time-dependent loading. Doan and Lee (2017) proposed non-spurious buckling mode scheme in computing buckling constraints based on multi-material topology optimization. Banh and Lee (2018) contributed a novel numerical and design approach to optimize topologies for cracked structures by using multi-material topology optimization method.

Regarding numerical simulations of improving structural performance for plate-like-structures, Goo *et al*. (2016) studied optimal topologies for thin plate structures with bending stress constraints to avoid the stress singularity phenomena. Yan et al. (2016) studied optimal topology design of damped vibrating plate structures subject to initial excitations. Belblidia *et al*. (2001) presented a novel topology optimization algorithm for Mindlin-Reissner plate structures with single and three-layered artificial material models. However, these studies did not consider variable materials as design variables. Variable materials with the same amount of total material may produce stiffer structures than single material (Zhou and Wang 2006, Tavakoli and Mohseni 2014). Therefore, the use of multiple materials may result in the superiority in terms of structural performance. In this study, the use of multiple materials in topology optimization of thin plate

∗Corresponding author, Associate Professor, E-mail: dongkyulee@sejong.ac.kr
[a] Ph.D. Student, E-mail: btthanhk11@gmail.com

http://www.techno-press.org/?journal=scs&subpage=6 ISSN: 1229-9367 (Print), 1598-6233 (Online)

structures by using classic plate theory is developed through computational simulation of Matlab (Doan and Lee 2017). In order to describe the phase of thin plate and resilient foundation, Pasternak type model is more realistic due to considering both the radial rigidity and the shear rigidity (Sheng and Wang 2008). Winkler type is a special case of Pasternak-type elastic foundation considering only the radial stiffness. Most plate structures are structural members that directly supported on the ground (Jung *et al*. 2014). Therefore, it is necessary to consider elastic ground effect of vertical pressure and shear layer effect. In this study, Pasternak-Winkler type elastic medium foundation is practically dealt with for multi-material topology optimization of thin plate. Moreover, both Winkler and Pasternak foundations are proposed to simulate the interaction between structures and elastic medium.

This study provides to engineers and designers an overview as well as a method how to evaluate both the mechanical and numerical interaction of thin plates with multi-material on elastic foundations within computational topology optimization. Multi-materials in a prescribed structure may result in the best structural performance within a mid-plate of thin plate and explain how to provide stress-path reinforcement and manufacture of mid-plate.

The contents of this study are organized as follows. The body of this paper begins in Section 2 with a brief description of finite element formulations for thin plate structures on elastic foundations based on classic plate theory. In Section 3, an analysis, design, and optimization model of multi-material topology optimization problem for thin plate structures are described. Stiffness formulation and sensitivity analysis of compliance are also presented in this section. Numerical examples considering the influences of the boundary condition, Winkler-Pasternak parameters and number of material are described in Section 4. Finally, conclusions are drawn in Section 5.

2. Finite element formulation of thin plates on elastic foundations

2.1 A brief of classic plate theory with elastic medium

To formulate governing equations of classic plate theory, a thin plate with the elastic medium is shown in Fig. 1. In this study, basic equations of Kirchhoff plate theory are summarized. Let Ω be the domain of a thin plate, $\partial\Omega$ is the boundary domain, and h is an uniform thickness. K_s and K_w denote shear layer foundation stiffness and Winkler foundation modulus of Pasternak model, respectively. Fig. 1 shows a thin plate embedded in elastic medium foundation by a so-called Pasternak model (Sheng and Wang 2008, Jung *et al*. 2014). A displacement field at any point of the plate is expressed as

$$u(x,y,z) = -zw_{0,x}(x,y) \tag{1a}$$

$$v(x,y,z) = -zw_{0,y}(x,y) \tag{1b}$$

$$w(x,y,z) = w_0(x,y) \tag{1c}$$

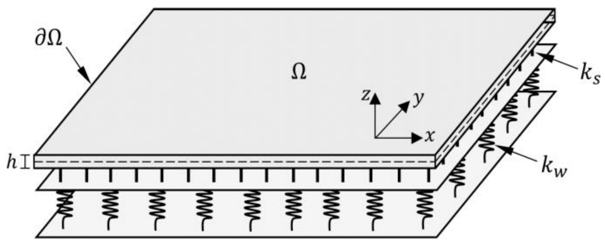

Fig. 1 Thin plate embedded in elastic medium which represented by Pasternak model

where w_0 is a component of displacement at a general point in a domain. By using Eq. (1), strains and moderate rotations according to strain-displacement relationship take the following form

$$\varepsilon_{xx} = -zw_{0,xx}, \quad \varepsilon_{yy} = -zw_{0,yy}, \quad \gamma_{xy} = -2zw_{0,xy} \tag{2}$$

The basic stress-strain (σ-ε) relationship of a plate structure in Cartesian coordinates x, y and z can be expressed in the following form

$$\left\{\sigma_{xx} \quad \sigma_{yy} \quad \sigma_{xy}\right\}^T = \begin{bmatrix} E_{11} & E_{12} & 0 \\ E_{21} & E_{22} & 0 \\ 0 & 0 & E_{33} \end{bmatrix} \left\{\varepsilon_{xx} \quad \varepsilon_{yy} \quad \varepsilon_{xy}\right\}^T \tag{3}$$

where

$$E_{11} = \frac{E_1}{1-\nu_{12}\nu_{21}}, \; E_{22} = \frac{E_2}{1-\nu_{12}\nu_{21}}, \; E_{12} = E_{21} = \frac{\nu_{12}E_2}{1-\nu_{12}\nu_{21}}, \; E_{33} = G_{12} \tag{4}$$

in which E_1, E_2 are Young's modulus and G_{12} is shear modulus. ν_{12} and ν_{21} are Poisson's ratio.

Substituting Eq. (2) into resultant moments (M_{xx}, M_{yy}, M_{xy}) = $\int_{-h/2}^{h/2} z\left(\sigma_{xx}, \sigma_{yy}, \sigma_{xy}\right) \mathrm{d}z$, one obtains

$$\left\{M_{xx} \quad M_{yy} \quad M_{xy}\right\}^T = \begin{bmatrix} D_{11} & D_{12} & 0 \\ D_{21} & D_{22} & 0 \\ 0 & 0 & D_{33} \end{bmatrix} \left\{\varepsilon_{xx} \quad \varepsilon_{yy} \quad \varepsilon_{xy}\right\}^T \tag{5}$$

where $D_{nm} = h^3E_{nm}/12$ with m, n = 1, 2, 3 is flexural rigidity.

By using the principle of virtual displacements for static problem, an equilibrium equation can be written as

$$M_{xx,xx} + 2M_{xy,xy} + M_{yy,yy} + q - p = 0 \tag{6}$$

where q is a distributed transverse load at surface; $p = k_w w_0 - k_s \nabla^2 w_0$ presents the reaction-deflection relation of Pasternak foundations.

By substituting Eqs. (2) and (5) into Eq. (6), the governing differential equation for bending plate can be written as

$$\begin{aligned} D_{11}w_{0,xxxx} + D_{22}w_{0,yyyy} + 2\left(D_{12} + 2D_{33}\right)w_{0,xyxy} - k_s\left(w_{0,xx} + w_{0,yy}\right) \\ + k_w w_0 - q = 0 \end{aligned} \tag{7}$$

By using Galerkin method (Zienkiewicz and Taylor 2013), multiplying with test function and integrating over the domain, a weak form of Eq. (7) can be obtained as

$$\int_{\Omega} A\mathrm{d}\Omega + \int_{\partial\Omega} A\mathrm{d}\partial\Omega = 0 \tag{8}$$

where

$$\begin{aligned} A = {} & D_{11}w_{0,xx}\phi_{,xx} + D_{22}w_{0,yy}\phi_{,yy} + D_{12}\left(w_{0,xx}\phi_{,yy} + w_{0,yy}\phi_{,xx}\right) + k_w w_0\phi \\ & + 2D_{33}w_{0,xy}\phi_{,xy} + k_s\left(w_{0,x}\phi_{,x} + w_{0,y}\phi_{,y}\right) \end{aligned} \tag{9a}$$

$$\begin{aligned} B = {} & \left(D_{11}w_{0,xxx}\phi - D_{11}w_{0,xx}\phi_{,x} - k_s w_{0,x}\phi + 2D_{33}w_{0,xyy}\phi - 2D_{33}w_{0,xy}\phi_{,y}\right. \\ & \left. + D_{12}w_{0,xyy}\phi - D_{12}w_{0,yy}\phi_{,x}\right)n_x + \left(D_{22}w_{yyy}\phi - D_{22}w_{0,yy}\phi_{,y} - k_s w_{0,y}\phi\right. \\ & \left. + 2D_{33}w_{0,xxy}\phi - 2D_{33}w_{0,xy}\phi_{,x} + D_{12}w_{0,xxy}\phi - D_{12}w_{0,xx}\phi_{,y}\right)n_y \end{aligned} \tag{9b}$$

2.2 Finite element implementation (Q4)

Polynomial coefficients can be expressed in terms of nodal coordinates and nodal degrees of freedom and then written as

$$w = \sum_{i=1}^{4}\left(N_{3i-2}w_i + N_{3i-1}w_{i,x} + N_{3i}w_{i,y}\right) = \sum_{j=1}^{12} N_j u_j \tag{10}$$

where N_i is the i-th Hermite function and $(u_{3n-2}, u_{3n-1}, u_{3n}) = (w_n, w_{n,x}, w_{n,y})$ with $n = 1, 2, 3, 4$.

Substituting Eq. (10) into the weak form of Eq. (8), a discretized system of element equation of thin plate can be expressed as

$$\sum_I K_{IJ} w_I = F_I \tag{11}$$

with

$$\begin{aligned} K_{IJ}^{(e)} = \int_{\Omega^{(e)}} \Big[& D_{11}N_{I,xx}N_{J,yy} + D_{22}N_{I,yy}N_{J,xx} + D_{12}\left(N_{I,xx}N_{J,yy} + N_{I,yy}N_{J,xx}\right. \\ & \left. + N_{I,yy}N_{J,xx}\right) + 2D_{33}N_{I,xy}N_{J,xy} + k_s\left(N_{I,x}N_{J,y} + N_{I,y}N_{J,x}\right) + k_w N_I N_J \Big]\mathrm{d}\Omega \end{aligned} \tag{12a}$$

$$F_I^{(e)} = \int_{\Omega^{(e)}} qN_I \,\mathrm{d}\Omega \tag{12b}$$

To calculate global deflection of plate $\mathbf{w}$, Eq. (11) can be reduced to the matrix form as follows

$$\mathbf{Kw} = \mathbf{F} \tag{13}$$

in which the stiffness matrix and force vector components are, respectively, defined

$$\mathbf{K}_{IJ} = \sum_{e=1}^{nel}\int_{\Omega^{(e)}} \mathbf{B}_I^{\mathrm{T}}\mathbf{D}\mathbf{B}_J \,\mathrm{d}\Omega; \quad \mathbf{F}_J = \sum_{e=1}^{nel}\int_{\Omega^{(e)}} q\mathbf{N}_J \,\mathrm{d}\Omega \tag{14}$$

with

$$\mathbf{B}_I = \begin{bmatrix} N_{I_1,xx} & N_{I_2,xx} & N_{I_3,xx} \\ N_{I_1,yy} & N_{I_2,yy} & N_{I_3,yy} \\ N_{I_1,xy} & N_{I_2,xy} & N_{I_3,xy} \\ N_{I_1,x} & N_{I_2,x} & N_{I_3,x} \\ N_{I_1,y} & N_{I_2,y} & N_{I_3,y} \\ N_{I_1} & N_{I_2} & N_{I_3} \end{bmatrix}; \quad \mathbf{D} = \begin{bmatrix} D_{11} & D_{12} & 0 & 0 & 0 & 0 \\ D_{12} & D_{22} & 0 & 0 & 0 & 0 \\ 0 & 0 & 4D_{33} & 0 & 0 & 0 \\ 0 & 0 & 0 & k_s & 0 & 0 \\ 0 & 0 & 0 & 0 & k_s & 0 \\ 0 & 0 & 0 & 0 & 0 & k_w \end{bmatrix} \tag{15a}$$

$$\mathbf{N} = \left\{N_1 \quad N_2 \quad N_3 \quad N_4 \quad N_5 \quad N_6 \quad N_7 \quad N_8 \quad N_9 \quad N_{10} \quad N_{11} \quad N_{12}\right\}^{\mathrm{T}} \tag{15b}$$

where $I_k = 3I + k - 3$ with $k = 1, 2, 3$.

3. Topology optimization formulation integrated with multiple materials

3.1 Multiphase topology optimization

Similar to topology optimization for single material, multi-material topology optimization is an optimization technique that seeks an optimal material layout under a given material invitation in a design domain by using multiple materials. It typically uses finite element method (FEM) and sensitivity analysis as an analysis model. We consider the minimum compliance based multi-material topology optimization problem within a design domain. Each subdomain Ω_k, $k = 1, 2, ..., n$ can be materials or voids in a design domain. Design schematic of multi-material topology optimization is shown in Fig. 2.

According to Bendsøe and Sigmund (2004), the void is considered as a separate material phase. In other words, multi-material topology optimization is to find the optimal material distribution of n number of materials corresponding to $n + 1$ material phases α_i at each point in a domain. In case of the minimum compliance based multi-material topology optimization problem, a modified SIMP version of linear interpolation is used within an elasticity stiffness tensor for multiple materials as follows

$$E(\alpha) = \sum_{i=1}^{n+1}\alpha_i^p E_i^0 \tag{16}$$

where p is a penalization factor. E_i^0 is a nominal elastic Young's modulus corresponding to phase i-th.

According to alternating active phase algorithm, multi-phase topology optimization problem is solved by converting multi-phase into $p(p-1)/2$ binary phases sub-problem. Each binary subproblem is a so-called active phase. In this process of each sub-problem, only two phases denoted as 'a' and 'b' are active at a time and the other phases are fixed. Overlaps of phases are not allowed in a desired optimal design, and then summation of the densities at each point $x \in \Omega$ should be equal to unity $\sum_{j=1}^{p}\alpha_j = 1$. The densities summation of two active phases at each

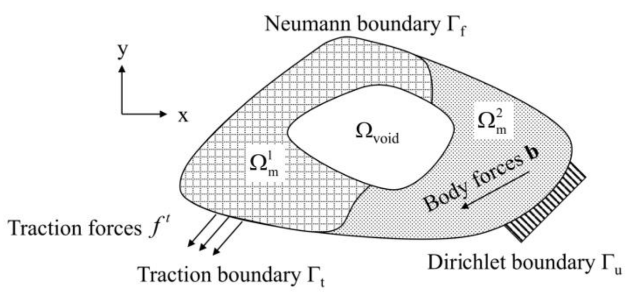

Fig. 2 Design domain for multi-material topology optimization

at each location for each sub-problem may be calculated as follows

$$\alpha_a(x)+\alpha_b(x)=1-\sum_{i=1,i\neq\{a,b\}}^{n+1}\alpha_i(x) \tag{17}$$

The general mathematical formulation of a structural multi-material topology optimization problem can be stated as follows

$$\begin{aligned} &\underset{\boldsymbol{\alpha}}{\text{minimize}}: && C\ (\alpha_i,\mathbf{U})=\mathbf{U}^{\mathrm{T}}\mathbf{K}\mathbf{U} \\ &\text{subject to}: && \mathbf{K}(\boldsymbol{\alpha})\mathbf{U}=\mathbf{F} \\ & && \int_\Omega \alpha_i dx \le V_i \\ & && 0<\varepsilon_i \le \alpha_i \le 1 \end{aligned} \tag{18}$$

where C is structural compliance. α_i is a density vector for phase material i-th. V_i is a per-material volume fraction constraint with $i = 1 : n + 1$ such that the summation should be equal to unity $\sum_i V_i = 1$. $\mathbf{U}$ and $\mathbf{F}$ are a global load and a displacement vector, respectively. $\mathbf{K}$ is a global stiffness matrix and $\boldsymbol{\Omega}$ is a given design domain. To avoid singularities in calculation processes of topology optimization, the problem is relaxed for densities between 0 and 1 through a very small lower bound non-zero value ε_i.

3.2 Compliance sensitivity formulation for thin plate on elastic foundation

From Eqs. (14), (16) and (18), element stiffness matrix components for multi-material topology optimization problem can be rewritten as follows

$$\mathbf{K}_{IJ}=\int_{\Omega^{(e)}}\mathbf{B}_I^{\mathrm{T}}\left(\sum_{k=1}^{n+1}\alpha_k^p\mathbf{D}_k^0\right)\mathbf{B}_J\,\mathrm{d}\Omega \tag{19}$$

where $\mathbf{K}_{IJ}$ of element e is a function of e-th density materials. $\mathbf{D}_k^0$ is a material property matrix of thin plate corresponding to the k-th phase material including Poisson's ratio v, a nominal elastic modulus E_k^0 and two Winkler-Pasternak parameters k_s, k_w.

$$\mathbf{D}_k^0=\begin{bmatrix} D_{11}^{0,k} & D_{12}^{0,k} & 0 & 0 & 0 & 0 \\ D_{12}^{0,k} & D_{22}^{0,k} & 0 & 0 & 0 & 0 \\ 0 & 0 & 4D_{33}^{0,k} & 0 & 0 & 0 \\ 0 & 0 & 0 & k_s & 0 & 0 \\ 0 & 0 & 0 & 0 & k_s & 0 \\ 0 & 0 & 0 & 0 & 0 & k_w \end{bmatrix} \tag{20}$$

where $D_{nm}^{0,k}=h^3E_{k,nm}^0/12$ with n, m = 1, 2, 3. The strain-displacement matrix is defined in Eq. (15a)

In terms of variable density, sensitivities of objective function are dependent on the sensitivity of the components. By using Eq. (17), sensitivity of elemental stiffness reflecting multi-material formulation in terms of design variables of multi-material densities can be written as follows

$$\frac{\partial\mathbf{K}_{IJ}}{\partial\alpha_a^e}=p\alpha_a^{p-1}\int_{\Omega^{(e)}}\mathbf{B}_I^{\mathrm{T}}\left(\overline{\mathbf{D}}_a^0-\overline{\mathbf{D}}_b^0\right)\mathbf{B}_J\,\mathrm{d}\Omega \tag{21}$$

where α_a^e is a density of phase 'a' of element e-th. Matrix $\overline{\mathbf{D}}_t^0$ is obtained by assigning value $k_s = k_w = 0$ for the matrix $\mathbf{D}_t^0$ with $t = \{a, b\}$. Finally, the sensitivities of objective function C and the material volume V in terms of multi-material densities can be written by using the adjoint equation as follows

$$\frac{\partial C}{\partial\alpha_a^e}=-\mathbf{U}_e^{\mathrm{T}}\frac{\partial\mathbf{K}^e}{\partial\alpha_a^e}\mathbf{U}_e \tag{22a}$$

$$\frac{\partial V}{\partial\alpha_a^e}=V^e \tag{22b}$$

where $\mathbf{U}_e$ and $\mathbf{V}_e$ are the displacement vector and the volume of element e-th, respectively.

In order to ensure existence of solutions to topology optimization problem and to avoid the formation of checkerboard patterns, a filtering technique on the resulting design is proposed by Bendsøe and Sigmund (2004). In this study, the filtered sensitivity of compliance $\partial C/\partial\alpha_a^e$ and material volume $\partial V/\partial\alpha_a^e$ with respect to density of phase 'a' of element e-th are derived as follows

$$\frac{\partial C}{\partial\alpha_a^e}=\frac{\sum_i H_{ei}\alpha_{ai}^e\dfrac{\partial C}{\partial\alpha_a^e}}{\alpha_{ai}^e\sum_i H_{ei}} \tag{23a}$$

$$\frac{\partial V}{\partial\alpha_a^e}=\frac{\sum_i H_{ei}\alpha_{ai}^e V^e}{\alpha_{ai}^e\sum_i H_{ei}} \tag{23b}$$

where $H_{ei} = r_{\min} - \mathrm{dist}(e, \{f \in \mathbb{N} : \mathrm{dist}\ (e, f) \le r_{\min}\})$ is a convolution operator. $r_{\min}$ is the filter radius and dist(e, f) is the distance between the center of element e and center of element f as shown in Fig. 3.

4. Numerical application and discussion

First, an accurate modeling test (Zienkiewicz 2000) of the non-dimensional central displacement of a square plate for several meshes is executed under uniform transverse pressure (P = 1) simply supported (SSSS) and clamped (CCCC) boundary conditions. The non-dimensional

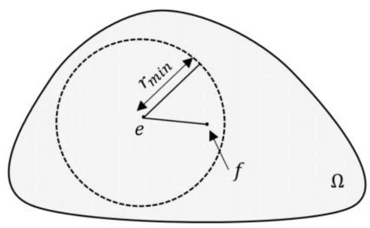

Fig. 3 Design domain for multi-material topology optimization

transverse displacement is set as $\overline{w} = \frac{wEh^3}{12Pl^4(1-v^2)}$. Fig. 4 verifies the accuracy of displacement models of thin plate.

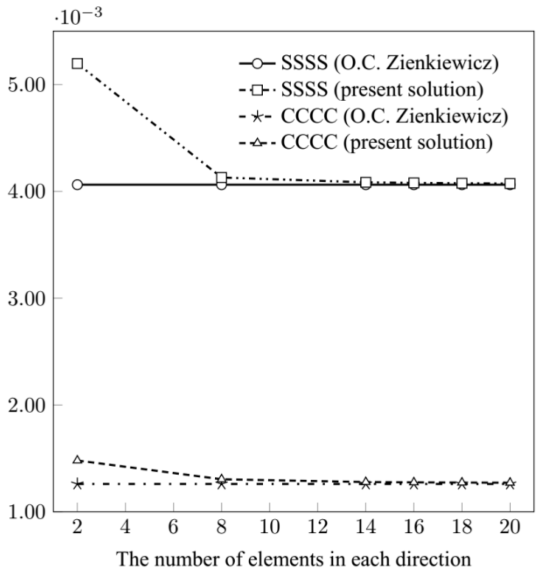

Fig. 4 Accurate modeling test results of the non-dimensional central displacement for two boundary conditions

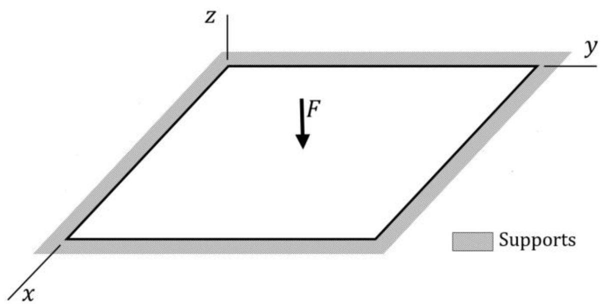

Fig. 5 Definition of load and boundary conditions in a design domain

Through the increase of element number, the present plate models converge to analytical solutions of Zienkiewicz (2000).

Next, two examples of a thin plate-like-structure subject to a bending load for multi-material topology optimization is dealt with. The design domain is modeled as a square plate finite element 20 × 20. The magnitude of force F = −1. The problem situation is shown in Fig. 5. The penalization factor for interpolating elasticity properties of stiffness is 3. Steel is one of popular material is used in construction industry. In the scope of this study, multi-steel materials topology optimization for thin plate on elastic foundations is investigated by using the Poisson's ratio 0.3. For all examples, plate dimensions are l_x = l_y = 1 and the plate's thickness equation h = 0.01 is used uniformly.

Optimized topology results are surveyed for dependency of various materials. The material is assumed to be isotropic. The total volume fraction is fixed to 40%. Young's modulus and volume fraction parameter for each material are presented in Table 1, where the indicators r, b and g denote red, blue and green colors, respectively. Note that Young's modulus and volume fraction of void material are, respectively, E_v = 10^{-4} and $V_v = 1 - \sum_{k \neq v} V_k$ for all examples.

4.1 Example 1: Optimized multi-material topology design with boundary condition dependency

Multi-material topology optimization of three different boundary conditions, i.e., fully clamped (CCCC), fully simply supported (SSSS) and clamped-free mixed (CFCF) boundary conditions is considered within the same amount of total material. The optimal topologies of thin plates in terms of the assignment of single and multiple materials are shown in Figs. 6-8. As can be seen, optimal topologies are varied depending on the number of material type and boundary conditions. Moreover, in three material case of SSSS as shown in Fig. 7, the material densities distribute at edge, opposite to results of one and two materials. It shows that depending on the number of materials and the kind of boundary condition, the distribution of topology

Table 1 Material properties for each material

Material properties	Number of materials		
	(a) One (red)	(b) Two (red, blue)	(c) Three (red, blue and gree)
Young's modulus	$E_r^0 = 1$	$E_r^0 = 1,\ \ E_b^0 = 2$	$E_r^0 = 1,\ \ E_b^0 = 2,\ \ E_b^0 = 3$
Volume fraction (40%V_0)	$V_r = 40\%$	$V_r = 10\%,\ \ V_r = 30\%$	$V_r = 5\%, V_r = 15\%, V_r = 20\%$

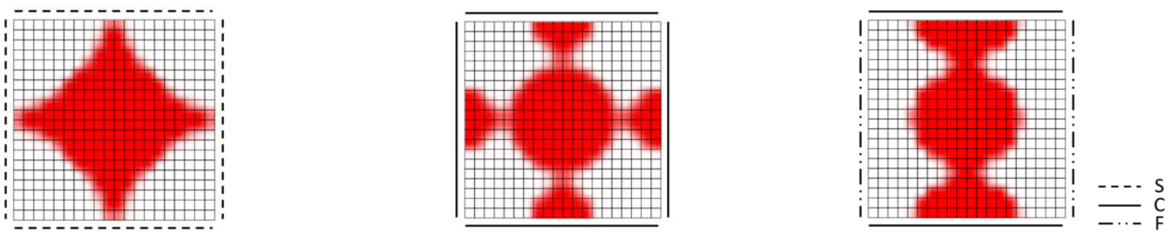

(a) SSSS, C = 302804 (b) CCCC, C = 107764 (c) CFCF, C = 156586

Fig. 6 Optimal topology results of thin plate by using single material

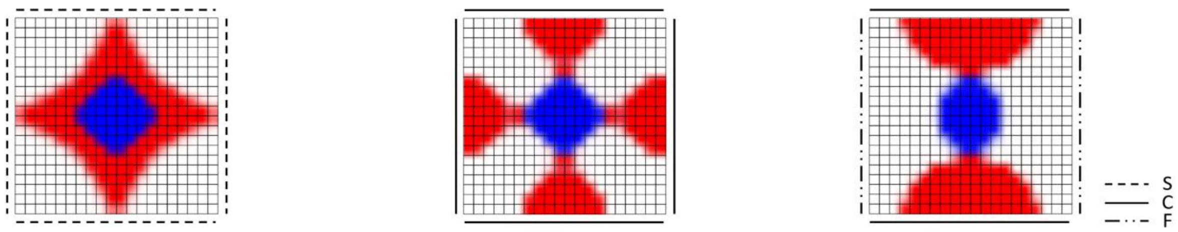

(a) SSSS, C = 286676 (b) CCCC, C = 88087 (c) CFCF, C = 131891

Fig. 7 Optimal topology results of thin plate by using two materials

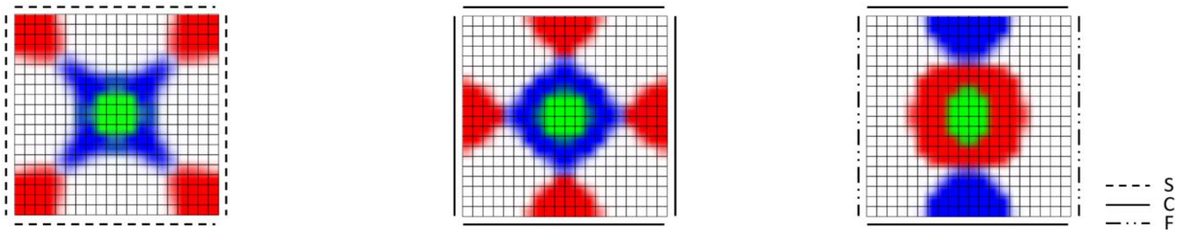

(a) SSSS, C = 276449 (b) CCCC, C = 70981 (c) CFCF, C = 93150

Fig. 8 Optimal topology results of thin plate by using three materials

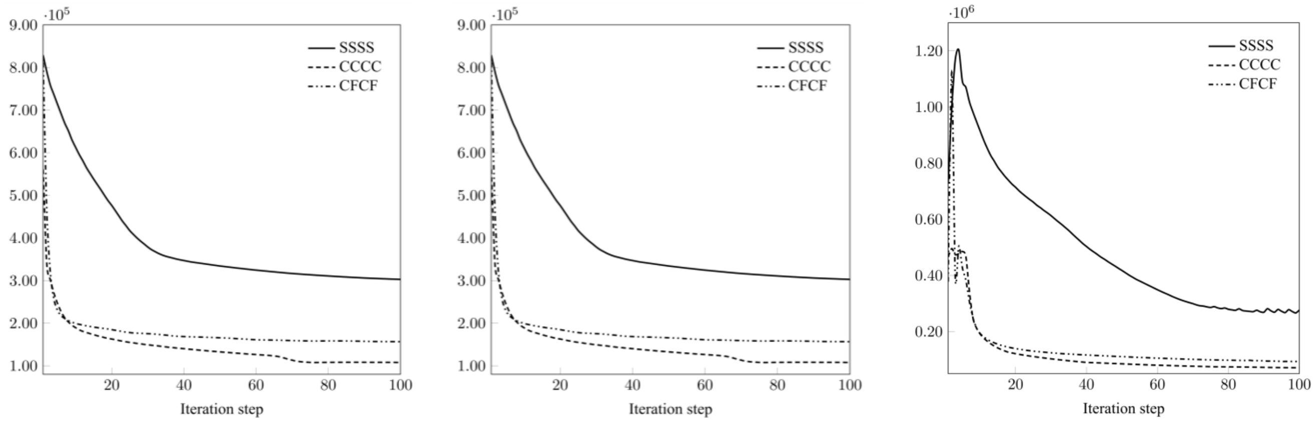

(a) Single material (b) Two materials (c) Three materials

Fig. 9 Convergence histories of objective function

optimization shape can be re-distributed to find the best topology optimal shape for structures. Stiff materials tend to automatically be assigned with strong stress concentration regions such as load and boundary positions. As can be seen in Fig. 9, the converged compliance in three material case of three different boundary conditions is the smallest of all cases. Especially the converged compliance in CCCC is always smaller than those of the rest case of boundary condition. It leads to produces stiff mid-plates.

4.2 Example 2: The effect of elastic medium parameters for optimized multi-material topology design

In this section, the effect of elastic medium for optimized topology results is investigated under the condition of single and multiple materials use CCCC condition is considered. For this purpose, the non-dimensional Winkler parameter K_W and the non-dimensional shear parameter K_S are defined as

$$K_W = k_w l_x^4 / D \tag{24a}$$

$$K_S = k_s l_x^2 / D \tag{24b}$$

The results presented in Fig. 10 describe the converged compliance values and optimal topologies with respect to different values of Winkler stiffness. Here, the non-dimensional shear parameter is taken zero. As can be seen, when the non-dimensional Winkler parameter is zero, it means that the plate is not affected by elastic foundation, the compliance is higher than other cases. Moreover, as the number of rigid materials increases, the convergence value of compliance decreases, and the optimal topology design start to re-distribute material densities in structure. Fig. 11 shows the effect of shear modulus parameter K_S

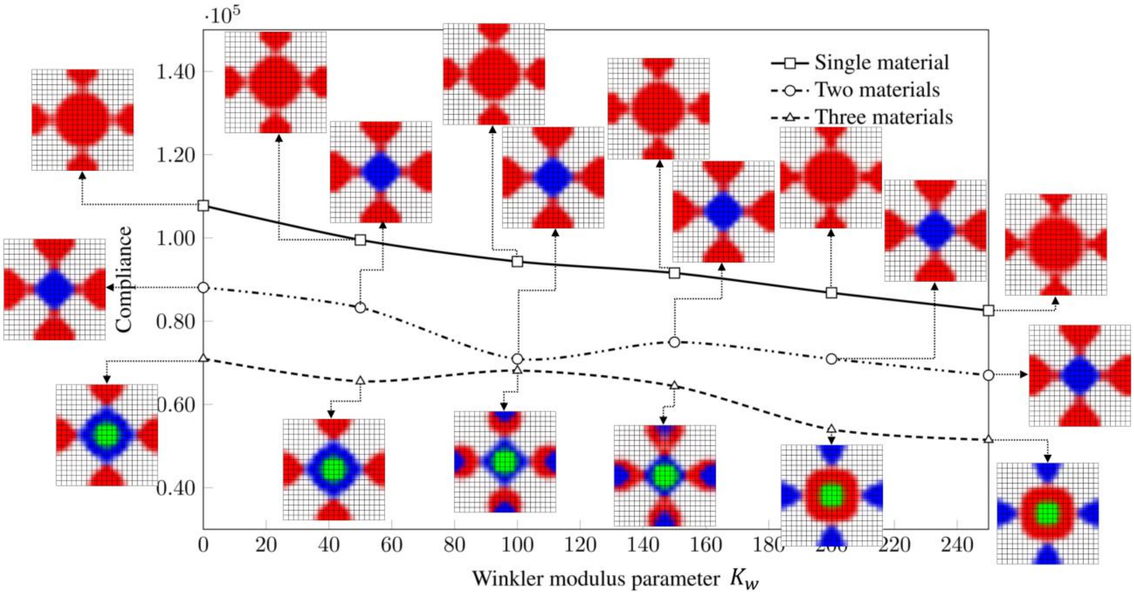

Fig. 10 Converged values of compliance and final optimal topologies in one to three materials thin plate (K_S = 0)

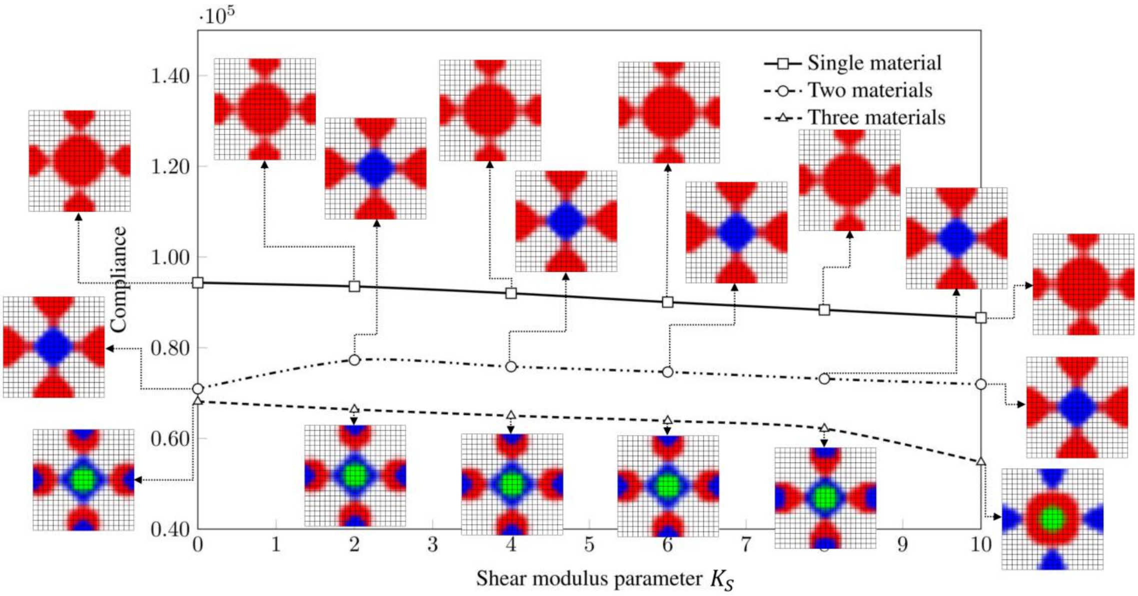

Fig. 11 Converged values of compliance and final optimal topologies in one to three materials thin plate (K_W = 100)

corresponding to K_W = 100. Similar to Fig. 10, when the number of material increases, the converged compliance decreases. As can be seen in Figs. 10 and 11, the increase in K_W or K_S generally results in the production of mid-plates with high stiffness. In order words, the enforcement of elastic medium foundation leads to stiff multi-material mid-plates.

5. Conclusions

In the present study, topology optimization for thin plates on elastic foundations based on the classic plate theory by using multiple materials is proposed. In the field of multi-material topology optimization, both Winkler and Pasternak-type foundation are developed to simulate the interaction between thin plate and elastic medium through computation software Matlab. Numerical examples verify the effect of boundary conditions, Winkler-Pasternak parameters, and the number of materials in optimal design of thin plate. Finally, optimal topology information of mid-plate of thin plate with elastic foundations effectively provides conceptual design to produce the thin plate to engineers and designers in this study.

Acknowledgments

This research was supported by grants (NRF-2017R1A2B4001960, 2017R1D1A1B03031350) from NRF

(National Research Foundation of Korea)) of Korean government.

References

Alonso, C., Ansola, R. and Querin, O.M. (2014), "Topology synthesis of multi-material compliant mechanisms with a Sequential Element Rejection and Admission method", *Finite Elem. Anal. Des.*, **85**, 11-19.

Banh, T.T. and Lee, D. (2018), "Multi-material topology optimization of design for continuum structures with crack", *Compos. Struct.*, **186**, 193-209.

Bendsøe, M.P. and Kikuchi, N. (1988), "Generating optimal topologies in structural design using a homogenization method", *Comput. Methods Appl. Mech. Eng.*, **71**(2), 197-224.

Bendsøe, M.P. and Sigmund, O. (2004), *Topology Optimization: Theory, Methods, and Applications*, SpringerVerlag Berlin Heidelberg, New York, NY, USA.

Belblidia, F., Lee, J.E.B., Rechak, S. and Hinton, E. (2001), "Topology optimization of plate structures using a single- or three-layered artificial material model", *Adv. Eng. Software*, **32**(2), 159-168.

Blasques, J.P. and Stolpe, M. (2012), "Multi-material topology optimization of laminated composite beam cross sections", *Mater. Des.*, **94**(11), 3278-3289.

Doan, Q.H. and Lee, D. (2017), "Optimum topology design of multi-material structures with non-spurious buckling constraints", *Adv. Eng. Software*, **114**, 110-120.

Du, Y., Li, H., Luo, Z. and Tian, Q. (2017), "Topological design optimization of lattice structures to maximize shear stiffness", *Advances in Engineering Software*, **112**, 211-221.

Goo, S., Wang, S., Hyun, J. and Jung, J. (2016), "Topology optimization of thin plate structures with bending stress constraints", *Comput. Struct.*, **175**, 134-143.

Jung, W.Y., Park, W.T. and Han, S.C. (2014), "Bending and vibration analysis of S-FGM microplates embedded in Pasternak elastic medium using the modified couple stress theory", *Int. J. Mech. Sci.*, **87**, 150-162.

Lee, D.K. and Shin, S.M. (2015), "Optimising node density-based structural material topology using eigenvalue of thin steel and concrete plates", *Mater. Res. Innov.*, **19**, 1241-1245.

Lee, D. and Shin, S. (2016), "Evaluation of Optimized Topology Design of Cross-Formed Structures with a Negative Poisson's Ratio", *Iran. J. Sci. Technol., Transact. Civil Eng.*, **40**(2), 109-120.

Lee, D., Shin, S., Lee, J. and Lee, K. (2015), "Layout evaluation of building outrigger truss by using material topology optimization", *Steel Compos. Struct., Int. J.*, **19**(2), 263-275.

Lee, D., Lee, J. and Doan, Q.H. (2017), "Multi-layered UL700 arch-grid module with inelastic buckling for localized reinforcement of soft ground", *Adv. Eng. Software*, **110**, 14-25.

Liu, Q., Chan, R. and Huang, X. (2016a), "Concurrent topology optimization of macrostructures and material microstructures for natural frequency", *Mater. Des.*, **106**, 380-390.

Liu, P., Luo, Y. and Kang, Z. (2016b), "Multi-material topology optimization considering interface behavior via XFEM and level set method", *Computer Methods in Applied Mechanics and Engineering*, **308**, 113–133.

Qiao, S., Han, X., Zhou, K. and Ji, J. (2016), "Seismic analysis of steel structure with brace configuration using topology optimization", *Steel Compos. Struct., Int. J.*, **21**(3), 501-515.

Roodsarabi, M., Khatibinia, M. and Sarafrazi, S.R. (2016), "Hybrid of topological derivative-based level set method and isogeometric analysis for structural topology optimization", *Steel Compos. Struct., Int. J.*, **21**(6), 1287-1306.

Sheng, G.G. and Wang, X. (2008), "Thermal vibration, buckling and dynamic stability of functionally graded cylindrical shells embedded in an elastic medium", *J. Reinf. Plast. Compos.*, **27**(2), 117-134.

Tavakoli, R. and Mohseni, S.M. (2014), "Alternating active-phase algorithm for multimaterial topology optimization problems: a 115-line MATLAB implementation", *Struct. Multidiscipl. Optimiz.*, **49**(4), 621-642.

Vatanabe, S.L., Lippi, T.N., de Lima, C.R., Paulino, G.H. and Silva, E.C. (2016), "Topology optimization with manufacturing constraints: A unified projection-based approach", *Adv. Eng. Software*, **100**, 97-112.

Xia, Q. and Wang, M.Y. (2008), "Topology optimization of thermoelastic structures using level set method", *Computat. Mech.*, **42**(6), 837.

Yan, K., Cheng, G. and Wang, B.P. (2016), "Topology optimization of plate structures subject to initial excitations for minimum dynamic performance index", *Struct. Multidiscipl. Optimiz.*, **53**(3), 623-633.

Yun, K.S. and Youn, S.K. (2017), "Multi-material topology optimization of viscoelastically damped structures under time-dependent loading", *Finite Elem. Anal. Des.*, **123**, 9-18.

Zhou, S. and Wang, M.Y. (2006), "3D multi-material structural topology optimization with the generalized Cahn-Hilliard equations", *Comput. Model. Eng. Sci.*, **16**(2), 83-101.

Zhou, S. and Wang, M.Y. (2007), "Multimaterial structural topology optimization with a generalized Cahn-Hilliard model of multiphase transition", *Struct. Multidiscipl. Optimiz.*, **33**(2), 89.

Zienkiewicz, O.C. (2000), *The Finite Element Method: Solid Mechanics*, Butterworth-Heinemann, United Kingdom.

Zienkiewicz, O.C. and Taylor, R.L. (2013), *The Finite Element Method: Its Basis and Fundamentals*, ButterworthHeinemann, United Kingdom.

CC